CONF-9606137--4
UCRL-JC-123514

Application of Soft X-ray Laser Interferometry to Study Large-scale-length, High-density Plasmas

A. S. Wan, T. W. Barbee, Jr., R. Cauble, P. Celliers,
L. B. Da Silva, C. Decker, J. C. Moreno, R. A. London,
P. W. Rambo, G. F. Stone, J. E. Trebes, F. Weber

This paper was prepared for submittal to the
5th International Conference on X-ray Lasers
Lund, Sweden
June 10-14, 1996.

May 1, 1996

Application of Soft X-ray Laser Interferometry to Study Large-scale-length, High-density Plasmas

A. S. Wan, T. W. Barbee, Jr., R. Cauble, P. Celliers, L. B. Da Silva, C. Decker, J. C. Moreno, R. A. London, P. W. Rambo, G. F. Stone, J. E. Trebes, F. Weber

Lawrence Livermore National Laboratory, P. O. Box 808, Livermore CA 94550

Abstract. We have employed a soft x-ray Mach-Zehnder interferometer, using a Ne-like Y x-ray laser at 155 Å as the probe source, to study large-scale-length, high-density colliding plasmas and exploding foils. The measured density profile of counter-streaming high-density colliding plasmas falls in between the calculated profiles using collisionless and fluid approximations with the radiation hydrodynamic code LASNEX. We have also performed simultaneous measured the local gain and electron density of Y x-ray laser amplifier. Measured gains in the amplifier were found to be between 10 and 20 cm^{-1}, similar to predictions and indicating that refraction is the major cause of signal loss in long line focus lasers. Images showed that high gain was produced in spots with dimensions of ~ 10 μm, which we believe is caused by intensity variations in the optical drive laser. Measured density variations were smooth on the 10-μm scale so that temperature variations were likely the cause of the localized gain regions. We are now using the interferometry technique as a mechanism to validate and benchmark our numerical codes used for the design and analysis of high-energy-density physics experiments.

1. Introduction

Recent demonstration of soft x-ray interferometry is a significant step in the measurement of 2-D n_e profiles of high-density, fast-evolving, and large scale length laser-produced plasmas [1], and allows for us to examine plasmas in ICF-relevant regime. Compare to conventional optical interferometers [2,3], we operate at 155 Å, using a collisionally pumped Ne-like Y (3p-3s) x-ray laser (XRL) [4] as the probe source, which allows us to obtain a two order of magnitude enhancement in spatial resolution due to reduced light refraction and more than a three order of magnitude enhancement in signal strength due to reduced absorption. The short pulse and high brightness of the XRL allowed us to obtain an interferogram in a single sub-200-ps exposure thereby reducing the effects of vibrations and motion blurring. The timing between the two Nova lasers, one to generate the XRL and one to produce the target laser plasma, was defined by the time-of-flight path of our interferometer setup and the desired probe time.

2. Colliding Plasma Experiment: Results and Data Analysis

The understanding of the collision and subsequent interaction of counter-streaming high-density plasmas is important for the design of ICF hohlraums [5]. In a typical indirectly-driven vacuum hohlraum, the interaction of the optical laser drive with high-Z inner surfaces generates counter-streaming plasmas which flow unimpeded and collide on the axis of cylindrically-shaped hohlraums. Single-fluid radiation hydrodynamics codes that we typically use to design ICF and other laser-plasma experiments, such as LASNEX [6], do not allow for plasma interpenetration. Without interpenetration, as the plasmas collide and stagnate, their kinetic energy converts to internal energy, resulting in unphysically large T_i which generates strong shocks that propagate away from the axis of symmetry. Furthermore, as the plasma stagnate

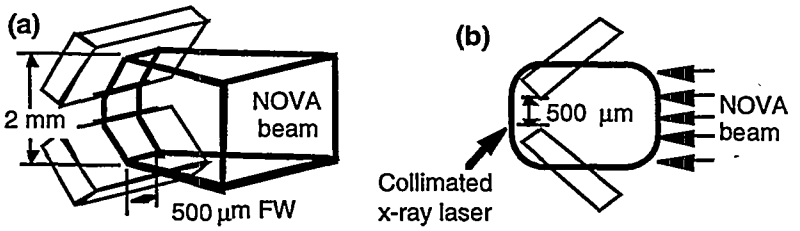

Fig. 1 The colliding plasma experimental setup. (a) 3-D view of Nova beam illuminating the 2 Au slabs. (b) side view showing the window of collimated XRL beam which defines the view of the gated detector.

on the hohlraum axis, single-fluid codes predict the creation of jets of high-velocity and high-density plasmas, which stream toward the capsule located at the center of the hohlraum and destroy the symmetry of the capsule implosion before capsule ignition.

The setup of our first colliding plasma experiment is shown in Fig. 1. Two Au slabs are aligned at 45 deg with respect to the symmetry axis with a minimum gap width of 500 μm between the tips of the slabs. A 500-μm full-width line-focused laser (1-ns squared with intensity of 3×10^{14} W/cm^2) incidents the slabs and generates two counter-streaming plasmas, which collide at late time. By varying the geometry, the slab materials, and the intensity of the incident laser, we can change the collisionality of the plasma. At high density and low temperatures, the plasma behaves like a fluid where codes like LASNEX should be able to model accurately. The plasma shifts into a collisionless region with increasing temperature and reducing density, where we expect to observe significant plasma interpenetration.

The target was backlit edge-on by the XRL (shown in Fig. 1b) starting at 1 ns after the start of the colliding plasma sequence. In Fig. 2 we show the measured interferogram of the colliding plasma with excellent fringe visibility. Near the symmetry axis of the two slabs we observe significantly greater fringe shifts as the results of the plasma collision and subsequent stagnation. We also observed self emission from the high density plasma near the slab surface. Using the unperturbed fringe pattern observed behind the slabs, where there is no plasma, we measure the amount of fringe shift due to the presence of plasma. The beamsplitters were not perfectly flat and that results in one of our experimental uncertainties. Based on previous null shots with similar quality beamsplitters, we estimate the uncertainty to be of order 0.1 fringe. Another source of the uncertainty is the path length across the target plasma in the direction of the collimated XRL beam can be significant since plasma expands in 3-D. [7] In this paper we assume a uniform plasma with a 500 μm path length, which is the transverse width of the optical laser line focus onto the Au slabs.

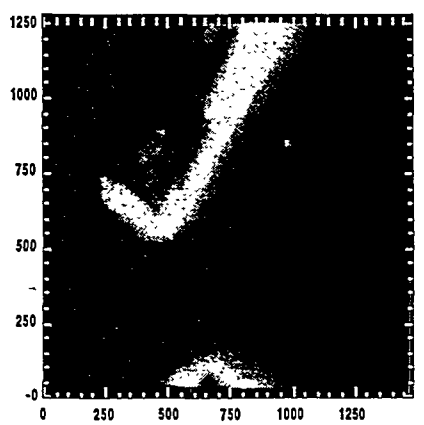

Fig. 2. Interferogram of the colliding plasma with excellent fringe visibility and self emission near slab surface. Extra fringe shifts on-axis is due to plasma stagnation.

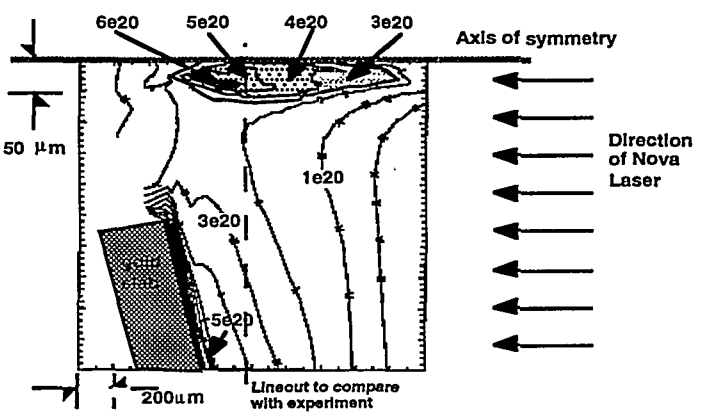

Fig. 3 Snapshot of a LASNEX-calculated 2-D n_e profile at a time of 150 ps after optical laser pulse. This time corresponds to the peak of the XRL pulse that served as the gate for our imaging detector used for the experiment.

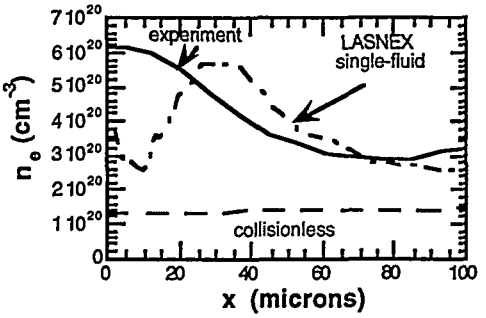

Fig. 4 Comparisons of measured (solid line) and calculated 1-D n_e profiles: LASNEX-calculated single-fluid profile (dashed-dotted line) and profile with a collisionless approximation (dashed line).

Fig. 3 shows a snapshot of a LASNEX-calculated 2-D n_e profile at 150 ps after the end of the optical laser pulse, which corresponds to the peak of the XRL pulse. This geometry simulates the lower half of the experiment with a mirror reflectivity boundary condition at the symmetry axis. In this calculation we use a multi-group radiation diffusion method. Neglecting the radiation opacity results in significantly lower temperatures. In the blowoff plasma, T_e is as high as 3 keV. Using the three temperature (T_e, T_i, and $T_{radiation}$) approximation where the radiation is assumed to be optically thin, LASNEX predicts a T_e of ~ 0.5 keV. As the blowoff plasma reaches the symmetry axis, the velocity of the zone boundary for a Lagrangian code is set equal to zero, and the slowing and stagnation of the counter-streaming single-fluid plasmas results in the conversion of kinetic to internal energy where T_i can reach a unphysically large values exceeding 10^3 keV. The resulting shock waves, whose intensity depends on the collisionality of the plasma, propagate away from the symmetry axis, as evident by the n_e peak off the symmetry axis.

Fig. 4 is a plot of 1-D cuts of the measured and calculated 2-D n_e profiles at 250 μm from the slab tip (at the minimum gap). Here we observed significant density increase on-axis due to the collision and stagnation with the measured n_e (solid line) as high as 6 x 10^{20} cm^{-3}. The observed stagnation region has a width of order 100 μm. Although LASNEX (dash-dotted line) predicts a comparable stagnation width, the n_e profile peaks at ~ 30 μm off the symmetry axis which is characteristic of the shock heated expansion predicted by LASNEX. In the collisionless regime where the plasma is hot and at low densities, n_e is the superpositioned density profiles from the two interpenetrating plasmas, which is shown as the dashed line in Fig. 3. At the symmetry plane the measured n_e is a factor of 3-4 higher than the n_e value in the collisionless regime The measured n_e profile falls in between the two calculated n_e profiles, representing the extremes of plasma collisionality. Incorporating plasma interpenetration in our predictive codes, such as multi-specie fluid codes [8] should significantly improve our predictive capability of laser-produced plasmas in a colliding configuration.

3. Exploding Foils: Simultaneous Measurement of Local Gain and n_e

Much XRL research effort has centered on the persistent inability to be able to model observed gain and spatial coherence properties; simulations over-estimate both features. Additionally, research has been directed toward enhancing XRL brightness and coherence. [9] Enhanced brightness has been achieved through improved target and experimental design, but the XRL remains spatially incoherent. [10]

Predictions of XRL performance start with a calculation of the local gain from an atomic model with level populations determined by expected conditions in the XRL plasma. For the Ne-like Y XRL, with the expected density at ~ 10^{21} cm^{-3} and the temperature near 1 keV, the calculated local gain is in the range of 10-20 cm^{-1}. Laser line trapping and radiation propagation with refraction, accounted for in full 2-D, time dependent hydrodynamic simulations, lower the average calculated gain to 10-11 cm^{-1} for few-cm-long XRLs. However, the average measured gain for the yttrium laser is still lower, ~ 5.3 cm^{-1}. [4]

One source of uncertainty has been the accuracy of the atomic kinetics calculations. This question has been here addressed here by using the XRL beam from a long, 3 cm, target to probe a short, 2 mm, XRL target which is driven in the same manner as the longer target. The short target acts as a one-pass amplifier of the incident probe from which the gain in the amplifier can be measured. [11] Since the amplifier is so short, there is negligible refraction of the lasing line. We have obtained the local gain profile with very high spatial resolution (1.3 μm). Also, we have performed the gain measurements using an interferometer which allows us to simultaneously measure the n_e profile. Both experimental features are necessary to conclude why measured XRL gain and coherence fall below predictions.

Fig. 2a is an end-on image of only the self-emission of a 2 mm Y target (no XRL backlighter and thus no interferometry). The foil is sitting at zero on the vertical scale and is irradiated from above by a 120 μm line focus along the line-of-sight. All that is visible is unstructured emission. The maximum number of counts per pixel is about 600 above background. Fig. 2b is an image of a 2 mm Y foil under the same drive conditions except that the foil is backlit by an Y XRL so that the foil plasma acts as an XRL amplifier. The data show strong amplification; the number of counts throughout most of the plasma is 10000 to 40000 above background. The local gain can be found from $I = I_o e^{gL} + I_o + I_S$, where I is the amplified intensity, I_o the incident intensity (equal to one-half the recorded background since the background is delivered through two arms of the interferometer), I_S, is the self-emission value taken from Fig. 2a, g is the gain and L is the amplification path length, 2 mm. The local gain was found to be 10-15 cm^{-1} in the central plasma, in general agreement with atomic models. The area of significant gain is limited to about 150 μm across the spot (horizontally) and from about -50 μm to about + 125 μm vertically.

The actual cause of the small-scale structure in the local gain, which is repeatable, is unknown, but we believe that it is the result of temperature fluctuations in the plasma. These temperature fluctuations are likely due to nonuniformities in the driving beam. As long as the driving beam is static over the time of peak gain, it is possible that such channels would not dissipate during the amplifying interval (~ 75 ps). Although laser-plasma instabilities, such as thermal self-focusing, can also give rise to small-scale filaments of high temperature plasma, this is an unlikely cause of the observed structure since we do not observe the density fluctuations associated with this mechanism.

The nonuniform structure also has a bearing on XRL coherence. As we have observed, the region of amplification in the XRL plasma is highly inhomogeneous. Since much of the gain is generated in small isolated regions, the spatial coherence of the XRL cannot be improved without smoothing the temperature field in the plasma. If the isolated gain structure is caused

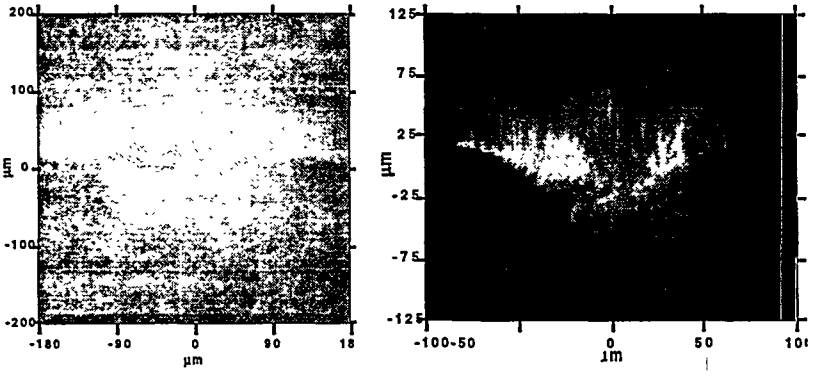

Fig. 2a: Image of self-emission of a 2-mm-long Y foil driven by a Nova line-focus laser beam with no XRL back-lighter.
Fig. 2b: Interferogram of a 2-mm-long Y foil. The light regions are areas of intense local amplification of the backlighting Y XRL. The plot is local gain along the lineout indicated on the image. The position of the lineout is noted by the bars on either side of the image.

by modulations in the driving laser, smoothing of the beam may alleviate the pockets and improve the spatial coherence of the XRL.

4. Summary

We have conducted a set of soft x-ray interferometry experiments for code validation and benchmarking. We studied the collision of high-density, high-temperature plasmas that is of interest to the design of ICF hohlraums. The measured n_e profile from two counter-streaming colliding plasmas peaks at the symmetry plane between the two slabs with a wide stagnation region. The peaked n_e values are a factor of 3-4 larger than the LASNEX-calculated values in a collisionless approximation with completely interpenetrating plasmas. Single fluid radiation Lagrangian hydrodynamics codes, such as LASNEX, do not allow for plasma interpenetration and predicts a unphysically large ion temperature and strong shocks propagating from the symmetry plane. The LASNEX-calculated n_e profile, in the signal fluid approximation, shows comparable stagnation width but with n_e profiles peaking off the symmetry plane, which is characteristic of strongly shock-heated, outward propagating plasmas.

We performed simultaneous measurement of local gain and n_e profiles of short laser-exploded Y foils, with near-1-μm resolution. Although the average measured local gain of ~ 10-20 cm^{-1} is in agreement with atomic models, and provides a validation of our atomic kinetic code, the gain profile is unexpectedly inhomogeneous. Intense gain occurs in regions of ~ 10 μm due, we believe, to modulations in the driving laser beam. This nonuniformity in gain may explain the disparity between measured and simulated gains for few-cm-long XRLs. In addition, it also explains the low level of spatial coherence observed.

The ultimate motivation of the development of soft XRL interferometry is to provide a mechanism to probe the deficiencies of our numerical model in areas such as laser deposition by both resonance and inverse bremsstrahlung absorption, flux-limited heat conduction, hydrodynamics, and non-local thermodynamics equilibrium atomic kinetics. The validation and benchmarking of the codes will allow us to gain better understanding of the physics of high-density laser-produced plasmas as we design more and more complex laser experiments for studying high-energy-density physics, and more specifically for hohlraum and capsule designs for ICF applications.

Acknowledgments

Work performed under the auspices of the U. S. DOE by LLNL under the contract number W-7405-ENG-48 and is partially supported by the Institute Sponsored Research Program.

References

1. L. B. Da Silva *et al.*, *Phys. Rev. Lett.* **74**, 3991 (1995).
2. R. S. Bosch *et al.*, *Phys. Fluids B* **4**, 979 (1992).
3. M. Prasad *et al.*, *Phys. Fluid B* **4**, 1569 (1992).
4. G. M. Shimkaveg *et al.*, *Proc. Soc. Photo-Opt. Instrum. Eng.* **1551**, 84 (1992); L. B. Da Silva *et al.*, *Opt. Lett.* **18**, 1174 (1993).
5. S. W. Haan *et al.*, *Phys. Plasmas* **2**, 2480 (1995).
6. G. B. Zimmerman and W. L. Kruer, *Com. Plas. Phys. and Cont. Fusion* **2**, 51 (1975).
7. A. S. Wan *et al.*, *J. Optical Society of America B* **13**, 447 (1996).
8. P. W. Rambo, J. Denavit, *Phys. Plasmas* **1**, 4050 (1994).
9. R. Kodama *et al.*, *Phys. Rev. Lett.* **73**, 3215 (1994); C.L.S. Lewis *et al.*, *Opt. Commun.* **91**, 71 (1992).
10. J. E. Trebes, *et al*, *Phys. Rev. Lett.* **68**, 588 (1992).
11. C. H. Skinner, *Opt. Lett.* **16**, 1266 (1991).